Eurasian Chemico-Technological Journal 16 (2014) 169-177

# Soot and Nanomaterials Formation in Flame

Z.A. Mansurov

The Institute of Combustion Problems, 172, Bogenbai Batyr St., 050012, Almaty, Kazakhstan

## Abstract

The seventieth anniversary of Professor Jürgen Warnatz is an important event for the scientific community of investigators of chemical kinetics and computation of combustion. His brilliant research in the field of combustion, particularly in the chemical kinetics reactions should be noted. His manuscript «Combustion» with co-authors is a handbook for specialists in the field of combustion and under my supervision was translated to Kazakh. Professor J.Warnatz contributed much to the development of combustion processes modeling and education of scientists from various countries, including Kazakhstan.

The general scheme of conversion of hydrocarbon fuels with new experimental data on the formation of fullerenes and graphenes, taking into account the pressure effect is proposed for the fuel-rich flames. It is shown that the formation of fullerenes is important to the corresponding spatial orientation of PAH, possible at low pressures. The formation of hydrophobic soot surface on silicon and nickel substrates during combustion of propane-oxygen flame was studied. It is stated that the hydrophobic properties are due to the presence of soot particles in the form of nanobeads.

***Keywords***: Soot, nanomaterials, fullerene, graphene, hydrophobic.

## Introduction

Simultaneously with the soot formation, fullerenes and nanotubes are formed by the mechanism competing with the mechanism of soot formation. Knowledge of the conditions and mechanisms of formation of soot, fullerenes, and nanotubes in flame allows one to change the combustion so that soot particles, fullerenes, or nanotubes are predominately formed.

At the present time a large number of experimental data on the processes of soot formation have been accumulated and different phenomenological models have been proposed [1, 2]. However, the mechanism of soot formation is imperfectly understood yet. This is explained by the fact that even in simple cases, such as the homogeneous pyrolysis of hydrocarbons, this process includes a large number of rapid simultaneous reactions leading to the formation of a new solid phase – soot particles (e.g., the time of transformation of methane with the molecular mass of 16 a.m.u into soot with the molecular mass more than $10^6$ a.m.u makes up $10^{-4}$–$10^{-2}$ s).

Considerable interest of scientific and technical communities to studying of production processes, structure and properties of nanosized systems is caused by variety and uniqueness of their practical applications. The small size of structural components – typically up to 100 nm – determines the difference in the properties of nanomaterials from massive analogues. Flame is a self-sustaining system in which hydrocarbons can be precursors of carbon nanomaterials, and the heat released during combustion, is a parameter of the process control. It is known that PAH are nucleation centers of forming soot i.e. PAH can be converted into either soot or fullerenes. The formation of CNTs occurs in diffusion flames from the fuel side and is initiated by particles of transition metals.

In accordance with general scheme, which was proposed previously by M. Frenklach [3] and H. Bockhorn [4] the precursor of soot formation is the formation of the first aromatic ring, polycyclic aromatic hydrocarbons, as well as nucleation of soot particles growth. In recent years, new data on formation of fullerenes [5-7], carbon nanotubes [8-10], superhydrophobic soot [11-13] and graphenes [14-16] in sooting mode were obtained. The works of J. Howard [17], H. Wang [18], A. Violi [19] and I.K. Puri [20] should be noted here.

---

* Corresponding author. E-mail: zmansurov@kaznu.kz

The $C_{60}$ and $C_{70}$ fullerene ions were detected in flames in 1987 and identified by the mass-spectrometry method [21]. Howard et al. [17] have obtained large amounts of $C_{60}$ and $C_{70}$ in laminar premixed soot forming flames of benzene and oxygen at low pressures. Unlike the evaporation of graphite, in the fullerenes formed in flames the ratio $C_{70}/C_{60}$ changes from 0.26 to 8.8 (in the case of evaporation of graphite, this ratio changes from 0.02 to 0.18).

It has been stated that in the soot at the front of a flame the number of structures with a closed shell as well as the concentration of the fullerene molecules in the gas phase increase with the increase in the time of their stay in this region. In the region located at the height of 70 mm above the burner, concentrations of fullerenes and structures with a closed shell are lower than those in regions located at heights of 60-120 mm. The highly ordered nanostructures, such as nanotubes and fullerene bulbs, were detected in solid samples taken from the walls and the upper part of the combustion chamber, which points to the fact that they are formed in the internal-redistribution processes occurring in the solid carbon during the time not longer than 100 ms [22].

Contrary to the supposition that fullerene structures are precursors of soot [23], the results of Grieco [24] point to the fact that a gas-phase growth of fullerene molecules along their vertical path in a flame takes place simultaneously with nucleation of soot particles and fullerenes are deposited on the growing soot particles.

Two ways of formation of fullerenes in flames were mainly discussed. Frenklach and Ebert [25] suggest that the number of the bent structures, i.e., PCAHs containing five- and six-membered rings, increase successively, which leads to the formation of fullerenes. They believe that the “bent” PCAHs are formed more rarely than the plane PCAHs in flames, which is in agreement with measurements of the concentrations of the PCAHs (including corannculene – a bent molecule) in the fullerene-forming flames [26].

As noted in [27], nano- and subnanosize particles are formed by gas-phase condensation in asymptotic giant branched stars. Experiments were carried out at pressures of 0.1–2.6 and 7 mbar, close to the values of $p$ in the astrophysical atmosphere at temperatures $T < 1\ 700$ K, at which the formation of fullerenes was observed.

The necessary condition for this mechanism is low pressure. As the pressure increases, i.e., with transition to atmospheric pressure or above, where triple collisions dominate, PCAHs coagulate to form soot clusters. It has been shown [28] that the maximum of fullerene formation is shifted to the right relative to the maximum of soot formation. In a detailed study of fullerene formation from benzene flames, the second maximum at 70 mm from the burner matrix was detected [29]. These data have provided the basis for the development of an alternative method of producing fullerenes in the hydrocarbon combustion regime.

Graphene consists of a single layer of $sp^2$-bonded atoms of carbon. Single and multiple layers of graphene have unique properties that represent a wide range of applications. There are various methods for synthesizing graphene (CVD-method, evaporation of SiC, mechanical exfoliation), however, the growth of graphene over large areas remains a challenge. Synthesis of graphene in the flame provides the ability to scale production. There are studies on the synthesis of graphene in a double flame and in the reverse flame [30] on copper and nickel substrates. However, production in the flame of at least three layers of graphene.

A new kinetic Monte Carlo [KMC] model has been developed by M. Frenklach [31], for graphene-edge growth, built on accumulated knowledge of elementary reaction processes. The model employs a more detailed description of surface reactions and sites and includes many more reactions creating five- and six-member ring complexes. Incorporation of five-member rings leads to graphene sheet curvature and so the KMC model is linked to a molecular mechanics (MM) geometry optimization to account for the resulting structures.

Representative graphene structures formed during growth of pyrene at 1500, 2000, and 2500 K are shown in [31]. At 1500 K, five-member rings are more stable than at higher temperatures and therefore are more frequently incorporated into the growing structures. The increased stability of five-member rings at lower temperatures has two affects on the growth of the layer. The first affect is promotion of growth through the creation of interior zipper growth nucleation sites. The second affect hinders growth as incorporation of five-member rings creates portions of edge that are unable to grow.

Five initial substrates were studied: pyrene, coronene, pentacene, decacene, and icosacene. The first two were allowed to grow on all sites and thus were used to simulate the initial stages of soot precursor growth. The last three are linear acenes of five, ten, and twenty rings, respectively. The linear species were used as models for graphene layer (soot surface) growth and hence the lower row of carbon atoms was set as solid type to keep them from reacting.

The original results on development of carbon nanomaterials of different functional application are presented in the article:

- Formation of soot and synthesis of fullerenes in flame;

- Formation of carbon nanotubes in flames;
- Formation of the hydrophobic soot in hydrocarbon flames;
- Formation of layered graphene films in the flames;
- Mechanism of soot formation in rich flames.

### *Formation of Fullerenes in Flame*

The structure of fullerene $C_{60}$ proposed by R. Smalley resembles a football, so it is sometimes called footballene, and that of $C_{70}$ resembles a rugby ball. Fullerenes $C_{60}$ and $C_{70}$ were identified in 1985 and prepared in macroscopic quantities in 1990, both by evaporation of graphite in an arc discharge [32]. In flames, fullerene ions were found in 1987, and in 1991, $C_{60}$ and $C_{70}$ were extracted in large quantities from laminar sooting flames of premixed mixtures of benzene and oxygen at low pressures [32] and then spectroscopically identified.

As noted in [27], nano- and subnanosize particles are formed by gas-phase condensation in asymptotic giant branched stars. The experiments were carried out at pressures of 0.1-2.6 and 7 mbar, close to the values of $p$ in the astrophysical atmosphere at temperatures $T < 1\ 700$ K, at which the formation of fullerenes was observed.

As fullerenes are formed at low pressures, the corresponding spatial orientation is important, which requires that the steric factor should be considered. For a molecule of $C_{60}$ to form, a spatial orientation of two molecules of $C_{30}$ is required. There are various models of formation of fullerenes $C_{60}$, one of which is the zip mechanism [33] (Fig. 1).

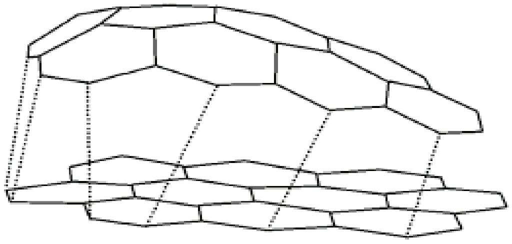

Fig. 1. Model of five- and six- membered rings through the connection of two PCAHs by the zip mechanism [27].

A necessary condition for this mechanism is low pressure. As the pressure increases, i.e., with transition to atmospheric pressure or above, where triple collisions dominate, PCAHs coagulate to form soot clusters. It has been shown [28] that the maximum of fullerene formation is shifted to the right relative to the maximum of soot formation. In a detailed study of fullerene formation from benzene flames, the second maximum at 70 mm from the burner matrix was detected.

The influence of gas discharge, the type of electrode, and the inter electrode spacing on the yield of fullerenes in combustion was studied. The experimental setup is shown in Fig. 2.

The experimental conditions were as follows: C/O = 1, $p$ = 40 torr [33], flow rate of benzene 250 $cm^3$/min, oxygen 758 $cm^3$/min, argon 101 $cm^3$/min, $v$ = 18.4 cm/s, $T$ = 1200 K, and $\delta$ = 0.5-0.8 cm; electrode systems are the needle-plane, plane-plane, and ring-plane with an inter electrode spacing of 4-21 cm; voltage $U$ = 0.5-20 kV. A premixed $C_6H_6/O_2/Ar$ flame under conditions corresponding to the maximum yield of fullerenes was studied [34].

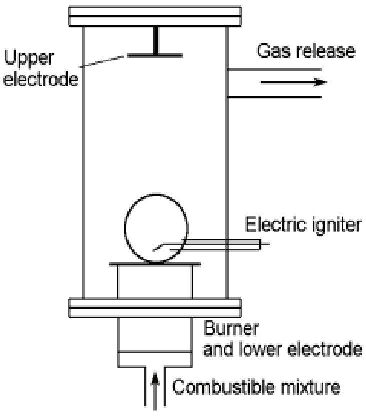

Fig. 2. The scheme of the setup.

Processing of the experimental data revealed the advantage of the ring electrode over the electrode in the form of a needle and showed that the yield of fullerene $C_{60}$ (≈15%) was the highest when the electrode was placed in the middle of the flame ($L$ = 4 cm). It has been found that if the peripheral zone of the benzene flame is heated by some external source, such as a laser beam, which not just burns the soot but also creates the same conditions as in the middle of the flame, the concentration of fullerenes increases. The effect of acetylene-oxygen flames on the different zones along the height of the benzene-oxygen flame has been studied using a ring burner. It has been found that fullerene formation is activated at the boundary of contact of the acetylene-oxygen and benzene-oxygen flames. The positive effect of the acetylene flame consists of increasing the temperature in the upper part of the reaction zone of the main benzene–oxygen flame by 50 ºC, increasing the degree of ionization, and intense conversion of PCAHs present in the benzene-oxygen flame to fullerenes [35].

The photographs of soot samples obtained with the use of a high-resolution JEM-3010 electron microscope of the JEOL firm with a magnifying power of up to 1.500.000 times at an accelerating voltage of 300 keV, show that these samples are highly structurized, which is characteristic of fullerene formations. It is known that the fullerenes formed in a flame are adsorbed, along with the polycyclic hydrocarbons, on the soot particles. The indicated photographs are presented in Figure 3 [36, 37].

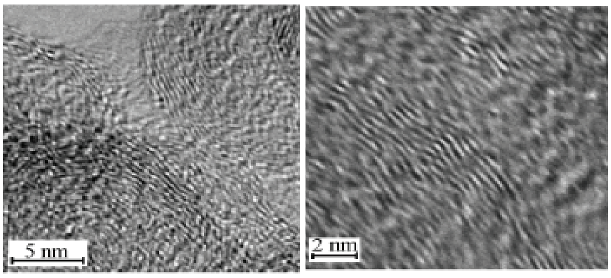

Fig. 3. Microscopic photographs of fullerene-containing soot samples obtained with different magnifying powers.

### *Formation of Carbon Nanotubes in Flames*

The most promising way to produce carbon nanotubes, according to Merchan-Merchan et al. [38], is the flame method. In the synthesis of carbon nanoparticles using flames, part of the fuel is consumed for heating of the mixture, and part is used as a reactant, which makes this method more cost-effective than methods based on the use of electricity, pyrolysis of hydrocarbons or arc evaporation of graphite.

Results of the study of a flat diffusion propane-oxygen flame stabilized on an opposed-jet burner at atmospheric pressure are presented in [39]. Two opposed flows formed a flat flame. The flame was surrounded by an external nitrogen flow supplied from the burner matrices. A solution of catalyst [$Fe(CO)_5$ or an alcoholic solution of nickel nitrate] was sprayed by an ultrasonic nebulizer and delivered through a metal nozzle into the flame from the side of the fuel. The conditions of the experiment are shown in Table. 1.

**Table 1**
Experimental conditions

| Catalyst | Flow rate of catalyst, cm$^3$/min | Gas flow rate, cm$^3$/min | | | | Flame temperature, ºC |
|---|---|---|---|---|---|---|
| | | $C_2H_2$ | $O_2$ | $N_2$ | $C_3H_8$ | |
| $Fe(CO)_5$ | 0.05 | 130-210 | 100-170 | 50-200 | - | 1700-1850 |
| $Ni(NO_3)_2{\cdot}6H_2O$ | 0.05 | - | 160-210 | 50-200 | 70-160 | 900-1150 |

The resulting products were deposited on the walls of the reactor and collected in traps with liquid nitrogen. The temperature in the reactor was measured by a thermocouple, and in the flame by an Iron Ultrimax pyrometer.

It is evident from Fig. 4 that the samples contain soot agglomerates, among which metal particles are encountered. It was found that under certain experimental conditions, well-ordered bundles of carbon nanotubes 20-30 nm in diameter formed.

The flame synthesis of carbon nanomaterials is mainly determined by carbon atoms serving as sources of graphite layers, the catalytic metals providing the transformation of the gas-phase carbon atoms into solid graphite layers, and the heat sources activating the catalytic metals. In [40], the synthesis of carbon nanotubes and nanofibres on a $Ni(NO_3)_2$ film deposited on a metal substrate with the use of a counter-flow ethylene flame as a heat source was investigated. Puri et al. have developed, on the basis of numerous experimental data on synthesis of carbon nanotubes in a flame, a model of formation of these nanotubes with participation of nanoparticles of the catalysts (Fe, Ni, Co) [20, 41, 42]. Figure 5a schematically described of the CNT formation process and in Fig. 5b shown schematic diagram of the CNT growth model by Puri and et al [20]. In this article [20] was underlined that the chemistry includes PAH species but soot was not modeled, since it has negligible presence in the flame.

In accordance with this model, nucleation of carbon nanotubes begins when the density of carbon atoms on the surface of the catalyst particles increases due to the addition of the indicated atoms from the outer shell of these particles. However, once the nucleation and growth of carbon nanotubes begins, carbon atoms are transported through the nanoparticles mainly due to their diffusion. This diffusion decreases with time because of the decrease in the concentration of the carbon atoms.

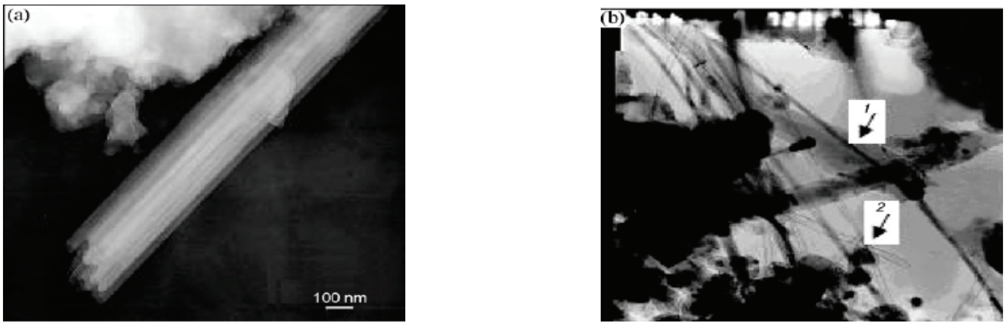

Fig. 4. Electron micrographs of samples: (a) carbon nanotube; (b) Ni in a carbon shell.

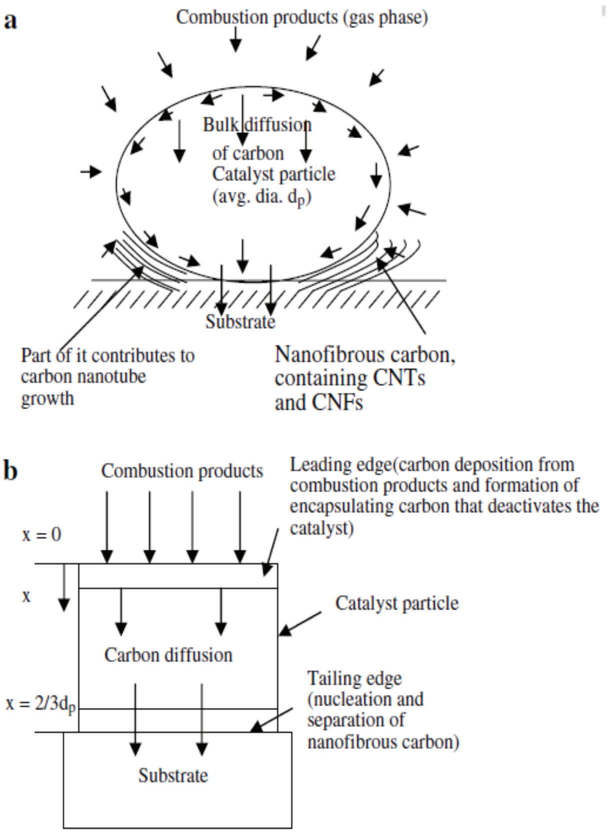

Fig. 5. (a) Schematic diagram of the CNT formation process. (b) Schematic diagram of the CNT growth model [20].

### *Formation of the Hydrophobic Soot in Hydrocarbon Flames*

Low surface-energy materials like amorphous carbon (a-C) films are frequently used to modify surfaces in order to control their wettability. The nanobeads are morphologically similar to the carbon nanopearls synthesized by Levesque and coworkers [43] by acetylene dissociation at 700 ºC on nickel catalyst nanoclusters. Puri et al. [44] have determined new ways of synthesis of carbon nanotubes in the fuel-rich diffusion flames, exposed to an electric field during 2-10 min, on superhydrophobic surfaces representing nanodimensional round amorphous carbon particles deposited on a silicon substrate [45].

A silicon (Si) disk is placed 2 cm above the burner, as shown in Fig. 6, and exposed to the flame for 4, 6 and 10 minutes. The nonpremixed flame is established using propane and oxygen flow rates of 50-150 cm$^3$/min and 260-310 cm$^3$/min. This resulted in the deposition of a carbon film, as shown in Fig. 6.

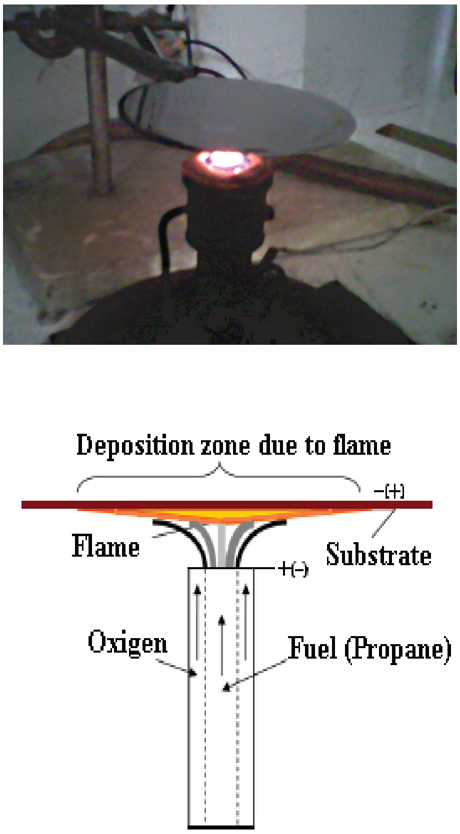

Fig. 6. Image and schematic representation of the burning experimental setup.

Si disc with a carbon nano-bead coating after a 4 min exposure to the flame showing the three deposition zones are shown in Fig. 7. The deposited carbonaceous material was examined using Raman spectroscopy. The Raman spectra of Fig. 7 for the middle zone was shown in Fig. 8 indicate the presence of several modifications of carbon. Raman peaks near 1350 $cm^{-1}$ (D – amorphous) and 1590 $cm^{-1}$ (G – graphite) in all three zones (1-3). However, what is new here is that the peaks near 1470 $cm^{-1}$ in Figs. 7a and 7b for Zones 1 and 2 are typical of fullerenes.

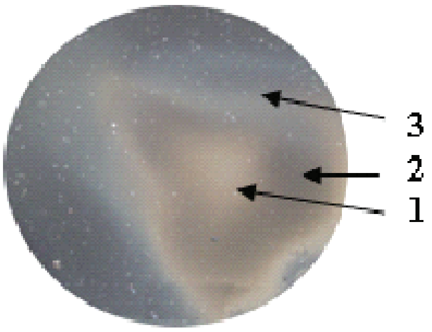

Fig. 7. A Si disc with a carbon nanobead coating after a 4 min exposure to the flame showing the three deposition zones.

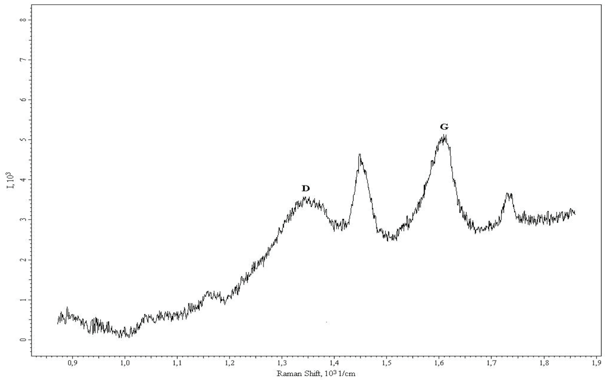

Fig. 8. Raman spectra of soot deposited on Si substrate; Ratio between the intensities of the G and the D peaks provides information about the lateral dimensions of the flakes.

It was investigated the influence of an electric field of 1 kV applied between the substrate and the burner rim. For studies the substrates were exposed with and without the applied field, in both cases for 10 min, to a flame established at propane and oxygen flow rates of 50 and 260 $cm^3$/min. For this flame, shown schematically in Fig. 6, middle zone contained carbon nano-bead chains that were 15-30 nm long in the absence of an electric field. The chain length was increased to 40-50 nm in middle zone when the electrical field was applied.

The formation of hydrophobic soot surface on silicon and nickel substrates during combustion of propane-oxygen flame was studied [45]. It is stated that the hydrophobic properties are due to the presence of soot particles in the form of nanobeads. A droplet of water on superhydrophobic soot is presented in Fig. 9.

Fig. 9. A droplet of water on superhydrophobic soot [45].

The results for the exploration of the soot formation of hydrophobic surfaces on silicon substrates and nickel during combustion of propane oxygen flame are listed. The distance from the burner matrix and the substrate was varied, the exposure time and the influence of the electric field of different polarity and voltage. It is shown that at the exposure of more than 4 minutes the soot with hydrophobic properties is formed and a division of the soot surface area occurs. The application of an electric field narrows the soot deposition on the substrate and in diameter of 2.5-3 cm from the centre; the soot super hydrophobic surface with a wetting angle of more than 1700 is formed.

## *Formation of Layered Graphene Films in the Flames*

Investigations on formation of layered graphene films were carried out in the propane-oxygen flame under the following conditions: flow rate of propane - 219.1 $cm^3$/min, the flow of oxygen – 438.2 – 313.0 $cm^3$/min, corresponding to the ratio of C/O = 0.75-1.05.

The studies were carried out both with the addition of argon in benzene-oxygen mixture in an amount of 300-650 $cm^3$/min and without argon. Copper and nickel catalytic substrates made of were used and placed in the flame. Varied range of residence time of the substrate in the flame: 5, 10, 20, 30, 40, 60 seconds, 5 and 10 min, the angle varied substrate relative to the vertical axis of the flame: $\alpha = 0, 30, 45, 60, 85$ °.

Flame temperature in the experiments was in the range 900-950 °. The sample formed on the substrate was examined for particulate structures by Raman spectrometer (NTEGRA Spectra).

It was found that a nickel substrate is more preferred for synthesis of graphene films. A copper substrate is an intensive formation of the amorphous structure of carbon black and copper oxides. Further studies were conducted on a nickel substrate.

The experimental results in the synthesis of the graphene layers of the premixed combustion of propane and butane-oxygen mixtures at various ratios of C/O are shown below. Argon consumption in all experiments was constant and is 250 cm$^3$/min. The results of the obtained minimum ratio IG/I$_2$D, characterize the amount of graphene layers on the substrate depending on the fuel source and the ratio C/O, and are presented in Table 2.

**Table 2**
The minimum $I_G/I_{2D}$ ratio depending on the ratio of C/O and fuel

| Corresponding to the ratio, C/O | 0.75 | 0.85 | 0.95 | 1.05 |
|---|---|---|---|---|
| Propane, $I_G/I_{2D}$ | 2.2 | 1.8 | 1.5 | 1.9 |
| Butane, $I_G/I_{2D}$ | 1.5 | 2.0 | 1.3 | 1.6 |

Figure 10 shows the Raman spectrum of the three layers of graphene, when placed in a flame of nickel substrate (C/O = 1.05; IG/I$_2$D = 1.6). It is found that the graphene layers are formed independently of the type of fuel in the studied range of ratios C/O with a pronounced peak of graphite G. The tendency for increasing the degree of disorder of the graphene layers according to increasing ratio of C/O, which are characterized by an increase in the peak intensity D. For propane-oxygen mixture the degree of disorder is observed at a higher ratio of C/O than for butane-oxygen mixture. However, butane-oxygen mixture at a ratio of C/O = 0.95 was obtained with the minimum number of graphene layers (three layers, IG/I$_2$D = 1.3) (Fig. 11).

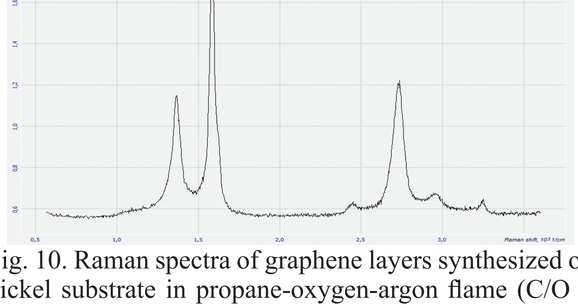

Fig. 10. Raman spectra of graphene layers synthesized on nickel substrate in propane-oxygen-argon flame (C/O = 0.95 and 1.05; $\tau = 5$ min), five layers – 1.05 ($I_G/I_{2D} = 1.6$).

### *Mechanism of Soot Formation in Rich Fflames*

The flame front structure of soot formation flames can be considered in close connection with mechanism of fuel conversion. A scheme suggested by M. Frenklach and H. Bockhorn [4] in 1994 is known, where polycyclic aromatic hydrocarbons (PAH) are precursors of soot particles.

Since then, in rich fuel flames the nanosized particles such as fullerenes and graphenes are found.

The fullerenes formation is generally observed at pressures below 60 Torr, because for fullerenes formation, an adherence of steric spatial factor, but in flames at atmospheric pressure this factor is prevented by triple collisions is necessary. Therefore, the pressure coordinate can be introduced to the general scheme for soot formation. At low pressure, formation of fullerenes from polycyclic aromatic hydrocarbon (PAH) occurs, but with increasing pressure, polycyclic aromatic hydrocarbons (PAH) coagulate to soot particles. The graphene is formed as intermediate product between PAH and soot particles, which is confirmed by the formation of multilayered graphene films at atmospheric pressure and single layered at the pressures below 60 Torr (Fig. 11).

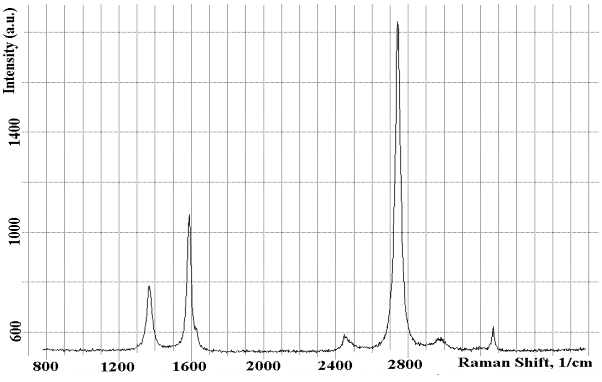

Fig. 11. Raman spectra of single-layer graphene samples obtained with the addition of benzene to $C_4H_{10}/O_2$ flame on a nickel substrate at a pressure of: 55 Torr ($I_G/I_{2D}$ = 0.58).

On the basis of the data on synthesis of fullerenes, carbon nanotubes, superhydrophobic soot and graphene in the flame it is possible to modify the general scheme proposed by H. Bockhorn [4] for rich fuel flames, namely to make a pressure-coordinate, which allows the formation of fullerenes at low pressures, and soot at high pressures. In addition the scheme was completed by graphene formation as an intermediate product stage of graphene formation (Fig. 12) [45].

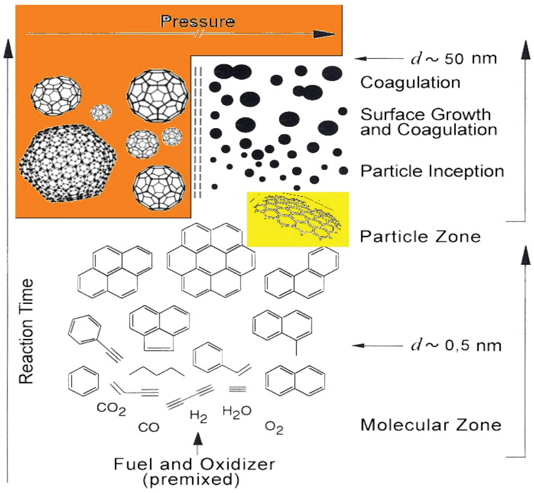

Fig. 12. Modified scheme for soot, fullerenes and graphene formation process in flames.

## References

[1]. B.S. Haynes, H.Gg. Wagner, Prog. Energy Combust. Sci., 7 (1981) 229–273.

[2]. K.H. Homann and H.G. Wagner, Some aspect of soot formation, in: J. Ray Bawen (Ed.), Dynamics of Exothermicity (Combust. Sc. Techol. Book Series, Vol. 2), Carbon and Breach Publishers (1996), P. 151–184.

[3]. M. Frenklach, H. Wang. Detailed mechanism and modeling of soot particle formation // Soot formation in Combustion. Springer-Verlag, Berlin, Heidelberg. 1994. P. 165–192.

[4]. H. Bockhorn (ed). Soot formation in Combustion. Springer-Verlag, Berlin, Heidelberg. 1994. P.4.

[5]. W. Kratshcmer, L.D. Lamb, K. Fostiropoulos and D.R. Huffman, Nature, 347 (1990) 354–358.

[6]. J.B. Howard, J.T. McKinnon, Y. Makarovsky, et. al. Prepr. Pap. Am. Chem. Soc. Div. Fuel. Chem. 36 (3) (1991) 1022–1025.

[7]. J.B. Howard. Proc. Combust. Inst. 24 (1992) 933–946.

[8]. S. Iijima, Nature 354 (1991) 56–58.

[9]. M.R. Falvo, R.M. Taylor, A. Helser et. al. Nature 397 (1999) 236–238.

[10]. W. Merchan-Merchan, A.V. Saveliev, L. Kennedy, W.C. Jimenez, Prog. Energy Combust. Sci. 36 (2010) 696–727.

[11]. S. Sen, I.K. Puri, Nanotechnology 15 (3) (2004) 264–268.

[12]. Y. Zhou, B. Wang, X. Song, E. Li, G. Li, S Zhao, H. Yan, Appl. Surf. Sci. 253 (5) (2006) 2690–2694.

[13]. M. Nazhipkyzy, B.T. Lesbayev, Z.A. Mansurov, N.G. Prikhodko, I.K. Puri. Synthesis of superhydrophobic carbon surface during combustion of hydrocarbons // World (Int.) Conf. on Carbon for Energy Storage / Conversion and Environment Protection «CESEP 2011»: – Vichy (France), 2011. – P. 154.

[14]. K.S. Novoselov, A.K. Geim, S.V. Dubonos et al. Physica E 12 (2002) 244–247.

[15]. K.S. Novoselov, A.K. Geim, S.V. Dubonos et al. Nature 426 (2003) 812–16.

[16]. N.G. Prikhodko, B.T. Lesbaev, M. Auyelkhankyzy, Z.A. Mansurov, Rus. J. of Phys. Chem. B, 8 (1) (2014) 61–64.

[17]. J.B. Howard, A.L. Lafleur and other, Carbon, 30 (1998) 1183–1201.

[18]. H. Wang. Pros. Combust. Inst. 33 (2011) 41–67

[19]. J.Y.W. Lai, P. Elvati, A.Violi. Phys. Chem. Phys., 16 (2014) P.7969.

[20]. S. Naha, S. Sen, A.K. De, and I.K. Puri, Proc. Combust. Inst., 31 (2) (2007) 1821–1829.

[21]. P. Gerhardt, S. Loffler and K.H. Homann, Proc. 22nd Int. Symp. Combust., The Combustion Inst., Pittsburgh (1988) 395-401

[22]. J.B. Howard, Fullerenes formation in flames, 24th Symp. (Int.) Combust., The Combustion Inst., Pittsburgh (1992), pp. 933–946.

[23]. H. Richter, A.J. Labrocca, W.J. Grieco, K. Taghizadeh, A.L. Lafleur, and J.B. Howard, J. Phys. Chem. B, 101 (1997) 1556–1560.

[24]. W.J. Grieco, J.B. Howard, L. C. Rainey, and J. B. Van der Sande, Carbon, 38 (2000) 597–614.

[25]. M. Frenklach and L.B. Ebert, J. Phys. Chem., 92 (1988) 561–563.

[26]. A.L. Lafleur, J.B. Howard, J.A. Marr, and T. Yadav, J. Phys. Chem., 97 (1993) 13539–13543.

[27]. C. JËager, F. Huisken, Jansa I. Lamas, Th. Henning. Astrophys., 696 (2009) 706–712.

[28]. J.B. Howard, 24th Symp. (Int.) Combust. (1992), pp. 933–946.

[29]. W.J. Grieco, A.L. Lafleur, K.C. Swallow, et al. Symp. (Int.) Combust. 27 (2) (1998) 1669–1675.

[30]. Z. Li, H. Zhu, D. Xie, et al. Chem. Commun., 47 (2011) 3520-3522

[31]. R. Whitesides and M. Frenklach. J. Phys. Chem. A, 114 (2010) 689–703.

[32]. H.W. Kroto, J.R. Heath, S.C. O'Brien, R.F. Curl and R.E. Smalley, Nature 318 (1985) 162-163.

[33]. J. Ahrens, M. Bachmann, Th. Baum, J. Griesheimer, R. Kovacs, P. WeilmËunster, K.-H. Homann, Int. J. Mass Spectrom. Ion Proc. 138 (1994) P.133–148

[34]. Z.A. Mansurov. Producing Nanomaterials in Combustion. Combustion, Explosion, and Shock Waves 2012; 48 (5):561–569.

[35]. Z.A. Mansurov, N.G. Prikhodko, T.T. Mashan, B.T. Lesbaev, Chem. Physics, 25 Vol. 10 (2006) 18–22.

[36]. Z.A. Mansurov, N.G. Prikhodko, B.T. Lesbaev, and T.T. Mashan, Proc. 31st Symp. (Int.) Combust., Heidelberg (2006), P. 164.

[37]. Z.A. Mansurov, T.A. Shabanova, V.L. Levin, and N.G. Prikhod'ko, A novel characteristic of a $C_{60}$–$C_{70}$- fullerene containing substance (according to electronic-microscopy data), Vestn. KazNU, Ser. Khimicheskaya, 39 (3) (2005) 444–448 (in russian).

[38]. W. Merchan-Merchan, A.V. Saveliev, L.A. Kennedy. Carbon 42 (3) (2004) 599–608.

[39]. Z.A. Mansurov. Adv. Mater. Res. 486 (2012) 134–139.

[40]. G.W. Lee, J. Jurng, and J. Hwang, J. Combust. Flame, 139 (2004) 167–175.

[41]. S. Naha and I.K. Puri, J. Phys. D: Appl. Phys., 41, No. 065304, 6 (2008).

[42]. S. Naha, S. Sen, and I.K. Puri, J. Carbon, 45 (8) (2007) 1702–1706.

[43]. A. Levesque, V.T. Binh, V. Semet, D. Guillot, R.Y. Fillit, M.D. Brookes, T.P. Nguyen. Thin Solid Films. 464-465 (2004) 308–314.

[44]. S. Naha, S. Sen, I.K. Puri. Carbon 45 (2007)1696–1716.

[45]. Z.A. Mansurov. Journal of Materials Science and Chemical Engineering, 2 (2014) 1–6.

*Received 17 March 2014*